Temperature Field Simulation and Process Parameter Optimization of Fiber Laser Assisted Turning Alumina Ceramics

Caizhou Xin[1], Haiyun Zhang[1,2*], Zhiguo Geng[1], Yanan Guo[1], Zengbo Zhang[1], Jinjian Zhang[1], Xu Miao[1], Yugang Zhao[1,2], and Xingang Han[1]
[1]*School of Mechanical Engineering, Shandong University of Technology, Zibo 255000, China*
[2]*Shandong Provincial Key Laboratory of Precision Manufacturing and Non-traditional Machining, Zibo 255000, China*
**Corresponding author's e-mail: zhy@sdut.edu.cn*

To explore the influence of laser-tool distance, laser power, spindle speed, and cutting depth on the surface quality of alumina ceramics, the turning test was carried out using fiber laser and CBN tool. The feasibility of the model is verified by temperature field simulation, and the range of process parameters is preliminarily determined, which provides a theoretical basis for further optimization. The response surface method was used to study the influence of the interaction of various processing factors on the test results, and the processing parameters were optimized and verified. According to the response surface analysis results, each process parameter's influencing factors on surface roughness are ranked as follows: cutting depth > laser power > spindle speed > laser-tool distance. Using the response surface methodology, the optimal machining parameters were determined with the objective of minimizing surface roughness. The optimal parameters obtained are as follows: the laser-tool distance is 0.95 mm, the laser power is 112 W, the spindle speed is 635 r / min, and the cutting depth is 0.22 mm. Conventional turning was conducted under optimal parameters to compare and analyze the surface morphology and tool wear between laser-assisted machining and conventional machining. Compared to conventional turning, the results demonstrate that laser-assisted turning significantly reduces surface roughness and cutting forces while improving surface quality and extending tool life. The minimum surface roughness reaches 0.806 μm and the average value reaches 0.816 μm after processing with optimized parameters.

DOI: 10.2961/jlmn.2025.02.2002
Keywords: laser-assisted cutting; alumina ceramics; response surface method; process parameters; surface roughness

1. Introduction

Alumina ceramics are a broad category with Al_2O_3 as its raw material. They are widely utilized in mechanical manufacturing, aerospace, and many other sectors due to their exceptional resistance to chemical corrosion, wear, oxidation, and other factors [1]. Alumina ceramics are difficult to process using traditional mechanical methods due to their extreme hardness and brittleness, which hinders improved surface integrity and significantly wears down turning tools [2, 3]. Laser-assisted machining and grinding are used to treat alumina ceramics [4]. The drawback of grinding is that it causes high-temperature thermal damage on the machined surface during the grinding and polishing process. Additionally, if the thermal damage layer is not sufficiently removed, it can cause cracks and plastic deformation on the material's surface and subsurface, significantly reducing the workpiece's service life [5]. Laser-assisted machining (LAM) is a typical high-temperature heat-assisted machining method in which laser beams are used before the turning tool comes into contact with the surface to be processed, so that the hardness of ceramic materials to reduce the fracture strength is higher than the yield limit, the material is sufficiently soft, and the tool can follow up on the removal of ceramic materials for plasticity turning [6-8]. Laser-assisted turning has the following advantages over traditional turning: reduced processing complexity, higher surface quality, reduced tool wear, and longer tool life [[9, 10].

Scholars discovered that LAM is effective for treating hard and brittle materials. Wang et al. used LAM to process Al_2O_3 particle-reinforced aluminum matrix composites. The results show that compared with traditional cutting, the cutting force of LAM is reduced by 30-50 %, the tool wear is reduced by 20-30 %, and the surface quality is improved [11]. Mohammadi et al. conducted experiments on Si (111) high-hardness materials, combined with single-point diamond tools for turning; the results show that laser-assisted thermal turning of Si (111) high-hardness material can obtain a better surface finish [12]. Kannan et al. used a high-intensity laser heat source for tensile heating research, and measured the thermal response of alumina ceramics to laser heating; the experimental results show that the surface temperature of alumina ceramics is mainly affected by laser power and laser scanning speed. When the surface temperature exceeds 850 °C, the turning force and tool wear decrease significantly [13]. Langan et al. used single-point diamonds as a tool for traditional turning and laser-assisted turning of sapphire. It was found that the fracture and spalling of the material after laser-assisted turning were alleviated, and the effect was extremely significant when the laser power was increased [14]. Jin et al. used a laser-assisted micro-milling method to soften materials by laser, expand the ductility domain of materials, improve the surface roughness of materials, and reduce tool wear. After processing, the surface roughness is effectively reduced to 51 nm, and the tool wear

width is reduced to 3.8μm [15]. Cao et al. studied the oxidation and ablation behavior of SiC ceramics by temperature field simulation and laser preheating experiments and determined the ablation critical temperature (1650°C) of the machined surface. By changing the laser power, three processing states and corresponding laser power ranges are determined, namely brittleness (0~185W), plasticity (185~225W), and thermal damage (>225W) [16]. Habrat et al. used AlTiN-coated tools to carry out LAM experiments on Ti-6Al-4V workpieces under different process conditions. They established a finite element model to study the time variation of the temperature field and the rate of heating and cooling. The results show that the martensite phase is formed at the top of the heat-affected zone of the workpiece, and the high temperature will lead to severe tool wear. A relatively high heating and cooling rate is observed with a smaller workpiece diameter and a lower cutting speed, proving that the martensite phase is produced by non-diffusion transformation [17]. Jeong and Lee combined LAM and heat shield to study the change in tool life and machining efficiency. After the combination, the tool life is improved and the heat energy applied to the tool by the laser heat source is reduced [18]. Pardha Saradhi et al. used fuzzy logic to predict the surface roughness and material removal rate (MRR) of alumina in LAM. The experimental values are in good agreement with the fuzzy model values and the model predicts surface roughness and MRR with a prediction error of 15.76% and 7.69% respectively [19]. Song et al. utilized a pulsed CO_2 laser beam to locally heat-fused silica and measured the surface roughness with a Taguchi orthogonal array. It was concluded that the pulse duty cycle was the main factor in achieving the minimum Ra value, and the removal mechanism of fused silica in the LAM was a mixture of quasi-plastic deformation and brittle fracture compared to conventional processing [20]. When Kuo et al. applied LAM to the machining of alumina ceramics, they found that LAM could drastically reduce the surface roughness of the material and greatly improve the material removal rate [21]. Bejjani et al. used LAM to process TiMMC under different cutting conditions and found that LAM can significantly extend tool life by up to 180 % [22]. In summary, LAM, as a new type of composite processing method, has obvious advantages in improving the machining performance of difficult-to-machine materials and will have broader applications in the field of high hardness and high brittleness materials.

In the processing of ceramic materials, especially bauxite ceramics (such as alumina ceramics), traditional machining methods often lead to significant tool wear, poor machining accuracy, and low surface quality due to their high hardness and brittleness. This not only limits their application in aerospace, medical, electronics, and other fields but also substantially increases production costs. To overcome these challenges, laser-assisted processing has been gradually proposed and applied to ceramic processing. Laser heating of ceramic surfaces can effectively reduce their hardness, thereby minimizing tool wear during processing and improving surface quality. However, existing research mostly focuses on a single processing parameter and lacks in-depth analysis of the interaction between multiple process parameters, such as laser power, tool-laser distance, and cutting depth. Therefore, this study investigates the laser-assisted turning of alumina ceramics using an established laser-assisted turning system. The objective of this study is to systematically analyze the process parameters of laser-assisted machining of ceramics using the response surface method (RSM), explore the interactions between these parameters, and optimize the machining process. The goal is to achieve more efficient and higher-quality ceramic processing, providing a theoretical foundation for industrial applications.

2. Experimental Testing Device and Materials

The laser-assisted turning experimental device is shown in Figure 1, which consists of a CNC horizontal lathe (CKD6136i, produced by Dalian Machine Tool Group) and a fiber laser heating unit. The fiber laser heating unit is mainly composed of a fiber laser generator (model YLR-150 / 1500-QCW-MM-AC-Y14, manufactured by IPG Photonics), an external optical path system, a laser fiber, and an external optical path system bracket.

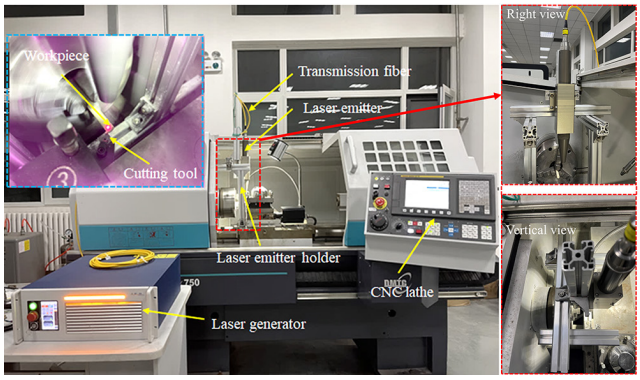

Fig. 1 Laser-assisted turning testing device.

A self-designed laser emitter holder supports the external optical path system. The support is adjusted along the feed direction to change the position of the laser output, and the corresponding spot position irradiated on the material's surface will change synchronously. In this process, the CBN tool is always kept at the original position of the tool holder, which in turn changes the distance between the laser spot and the tooltip. The processing principle of laser-assisted hot turning is illustrated in Figure 2. Before the turning tool engages, the laser beam first irradiates the surface of the alumina ceramic to be processed. The high-energy laser generates thermal energy that softens the material, reducing its hardness and increasing its fracture strength beyond the yield limit. Once the material is sufficiently softened, the high-temperature-resistant turning tool immediately removes the ceramic material through plastic deformation.

The material used in the experiment is a 99-type Al2O3 cylindrical workpiece, which is formed by isostatic sintering. The workpiece is an industrially purchased pre-machined blank, with its original surface subjected to conventional rough grinding (Ra approximately 1.5–2.0 μm). The size of the workpiece is φ10mm×100mm. The main performance parameters of type 99 Al_2O_3 ceramics are shown in Table 1. The turning tool used is a CBN tool with double-sided CBN inserts of type WNGA080408 and a 95° external turning tool holder of type MCLNR2020K12. A three-dimensional digital microscope (DSX1000, OLYMPUS, Japan) was used to collect surface roughness.

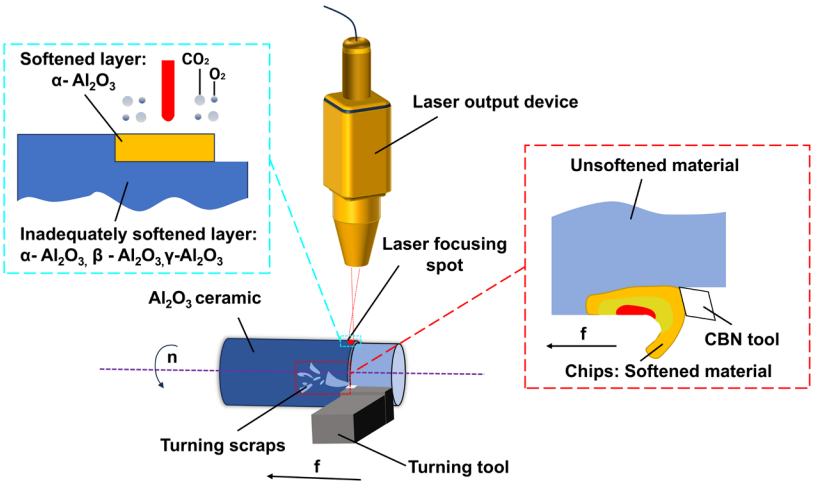

Fig. 2 The processing principle of laser-assisted turning

Table 1 99 Type Al_2O_3 ceramics main performance parameters.

Parameter	Parameter value
Material density（g/cm^3）	3.8
Rockwell hardness HRA	⩾89
Bending strength（MPa）	340
Thermal expansion coefficient（10^{-6}/℃）	7.7
Resistivity（Ω·mm^2/m）	>10^{14}
Thermal conductivity（W/m K）	29

3. Temperature field simulation

3.1 Heat Transfer

The laser heat source uses a Gaussian distribution, with the thermal flux density on the workpiece surface following a Gaussian profile and no internal heat generation during the process. ANSYS APDL was used to decompose the heat source vector into the x, y, and z directions at a specific point on the workpiece surface. The thermal flux density loading equation is expressed as follows:

$$Q_{(r)}=\frac{2P}{\pi R_G^2}\exp\left\{-3\frac{[x-R\times\cos(time\times v/R)]^2+[y-R\times\sin(time\times v/R)]^2+(z-f\times time)^2}{R_G^2}\right\}, \quad (1)$$

where R is the radius of the processed material [mm]; v is the linear velocity of laser heat source scanning [r/min]; f is the transverse feed rate of laser heat source [m/min]; P is the laser power [W]; R_G is the spot radius [m]; $Q(r)$ is the heat flux density on the boundary surface at r from the heat source center [W/m^2].

In laser-assisted heat treatment of alumina, heat conduction is the primary mode of heat transfer, with thermal convection and thermal radiation being neglected. Given that the temperature of the workpiece during laser-assisted turning exceeds 1000°C, the influence of heat generated by the tool on the temperature field is negligible compared to the heat from the high-temperature laser source. The model employs a second boundary condition, where the heat flux on the boundary is known. The temperature field simulation software translates this into a surface temperature map based on material properties, allowing for the assessment of whether the temperature meets processing requirements by analyzing the temperature map.

3.2 Model building and grid differentiation

As illustrated in Figure 2, the hardness of Al_2O_3 ceramics varies with temperature [21]. At 500°C, the hardness decreases to approximately half of its room temperature value, although it remains relatively high. When the temperature reaches 1000°C, the hardness of the material drops to 4.6 Gpa, which is about one-third of its room temperature level. At this elevated temperature, changes in the material structure occur, including the transition of the glass phase and the onset of plastic deformation. Consequently, turning operations in the softening layer can effectively remove material plasticity. The region where the axial and radial temperatures reach 1000°C is designated as the softening layer. The model is defined as a cylinder with a diameter of 10 mm and a height of 10 mm and is segmented into three distinct layers: the softened layer, the insufficiently softened layer, and the unsoftened layer. For grid division, the region with the outermost thickness of 1 mm is refined, with a grid size of 0.2 mm. The grid in the deeper regions, further from the surface of the workpiece, is slightly coarser. The total number of grid nodes is 254,909. The geometric model and grid division are illustrated in Figure 4. Grid quality assessment reveals an average grid quality of 0.93646 for the simulation. A grid quality value closer to 1 indicates better grid quality. Values above 0.7 suggest that the grid division is reasonable, reflecting good grid quality.

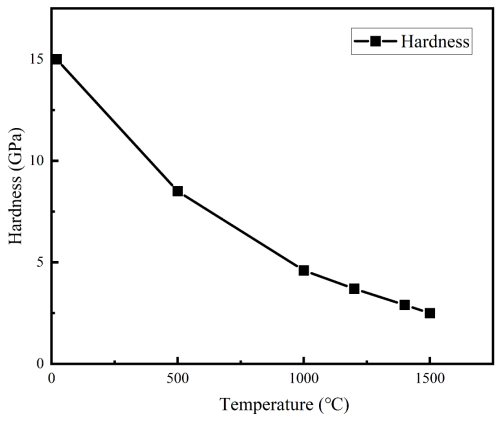

Fig. 3 Hardness of Al_2O_3.

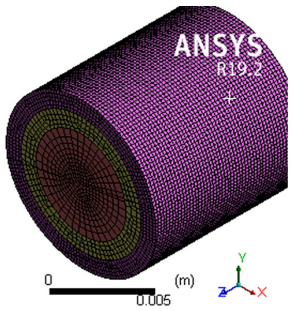

Fig. 4 Grid division diagram.

3.3 Single-factor temperature field simulation

In the temperature field simulation of laser-assisted turning, the influence of laser power and feed speed on temperature is mainly concerned. The laser power directly affects the heating intensity of the material surface. The higher the power, the faster the temperature rises. The feed rate determines the time when the laser irradiates the material. The slower the feed rate, the longer the material is exposed to the laser, resulting in a temperature rise. By adjusting these two parameters, the temperature distribution of the material during the machining process can be effectively controlled.

3.3.1 Laser power

In laser-assisted turning, the Al_2O_3 workpiece requires an adequate laser heat source to soften the material effectively. Adjusting the laser power represents the most straightforward method for altering the energy of the laser heat source. As illustrated in Figures 5 and 6, at a spindle speed of 300 r/min, a heat source diameter of 1 mm, and a feed speed of 4 mm/min, the maximum temperature, as well as the surface and radial temperature distribution of the workpiece, are recorded for various laser power levels (P).

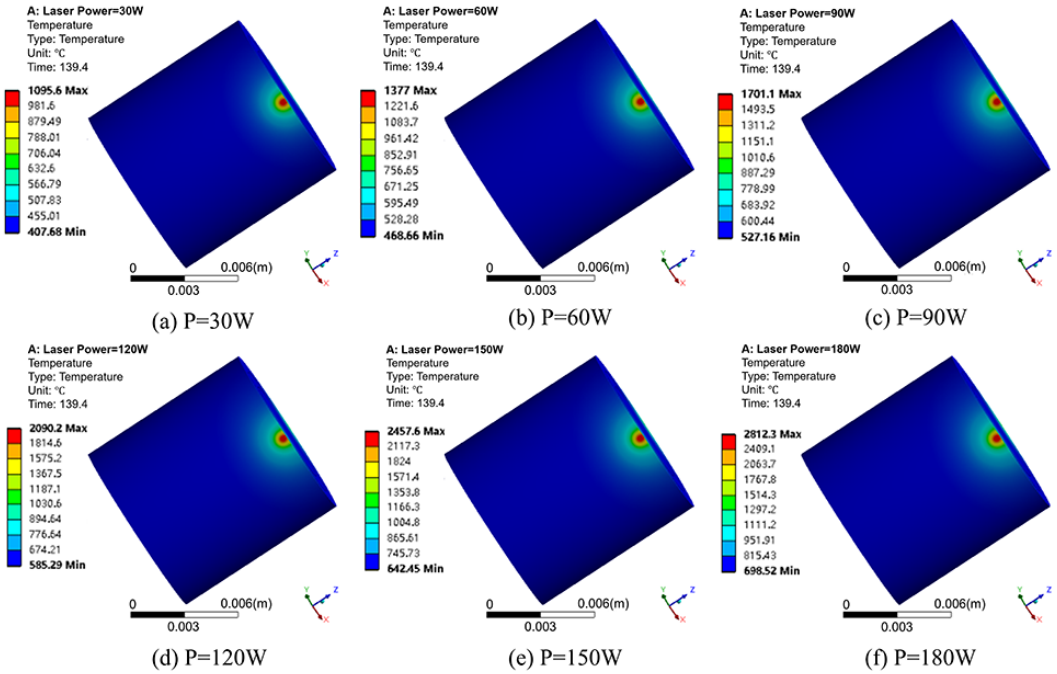

Fig. 5 Surface temperature under different laser power.

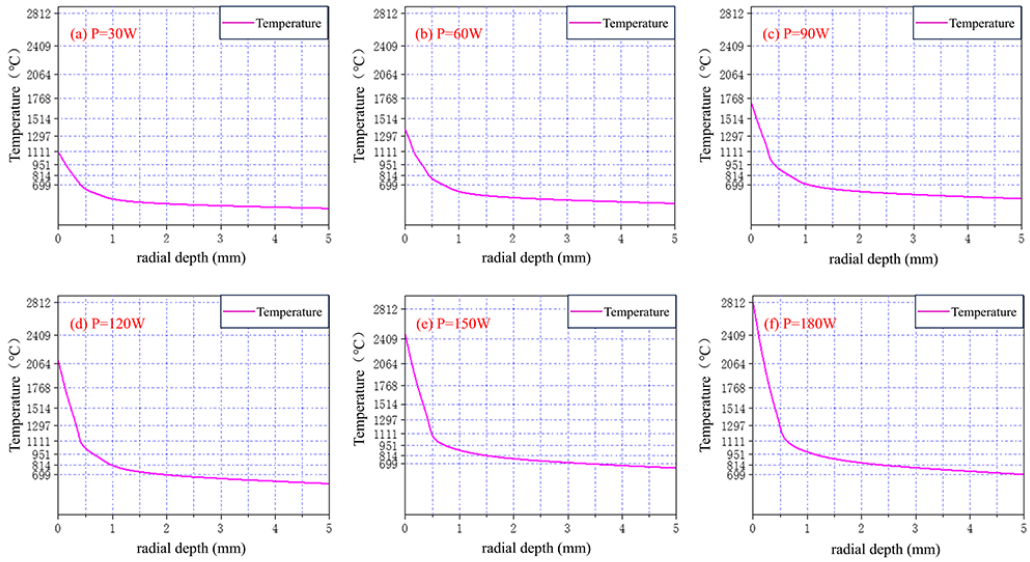

Fig. 6 Radial temperature at different laser power.

As the laser power increases, the temperature gradient between adjacent isotherms also intensifies. At a laser power of 30W, the maximum surface temperature of the material reaches 1095.6°C, which is just above the critical threshold for plastic deformation of 1000°C. When the power is raised to 180 W, the surface temperature escalates to 2812.3°C, significantly surpassing the melting temperature. Consequently, at this power level, it is crucial to employ a deeper back-cutting depth to avoid the melting of the material's surface.

Figure 6 demonstrates that this power level's softening depth is approximately 0.55mm. In theory, plastic removal can occur when the turning depth is less than 0.55mm; however, since the temperature exceeds the melting point, excessively shallow depths may lead to surface melting. Therefore, the actual turning depth should be maintained close to 0.55mm for optimal results. Additionally, the curves illustrate that higher power settings produce a steeper temperature gradient and a deeper high-temperature material layer, with the softening layer expanding as the power increases.

3.3.2 Feed speed

In laser-assisted turning, the laser beam and the turning tool feed axially at the same feed rate. The feed rate determines the time the laser irradiates the material within the unit processing length. At the same laser power and rotation speed, the lower feed rate requires a longer processing time to remove the same size of material, and a longer processing time will cause the laser to produce a higher temperature on the material's surface.

As shown in Figure 7, when the feed speed is 9 mm/min, the laser power is maintained at 180 W, the spindle speed is maintained at 300 r/min, and the surface temperature distribution of the material is maintained at different laser loading time points. The temperature rise of the material at the latter loading point is faster, so the material preheating link is set in the actual test to increase the temperature rise of the material at the initial stage.

Under different feed speeds, the laser power is maintained at 180 W, the spindle speed is 300 r/min, and the maximum surface temperature of the material is shown in Figure 8. With the increase of feed speed, the maximum surface temperature of the material decreases from 2684.1℃ to 1514.7℃, which reaches the critical temperature of material hardness decrease. The radial temperature distribution of the material also changes accordingly, and the size of the material layer that achieves the softening effect becomes smaller. Although the fast feed speed shortens the processing time, it has a great impact on the heat degree of the material, as depicted in Figure 9.

3.4 Temperature field verification

In laser-assisted turning, the radial temperature distribution determines the size of the softened layer of the material, while the maximum surface temperature of the temperature field dictates whether the material can be softened for plastic deformation. The cutting depth is selected based on the simulation results of the temperature field, followed by turning experiments to validate the reliability of these simulation outcomes.

Laser powers of 60, 90, 120, and 150 W were selected while maintaining a spindle speed of 300 r/min, a heat source diameter of 1 mm, and a feed rate of 4 mm/min. The cutting depth was determined based on the temperature field simulation results, and four cutting depths were chosen near the optimal value for experimentation. Results were evaluated based on surface roughness and material removal rate. Theoretical material removal rate (Q_T) and actual material removal rate (Q_P) were calculated using Equations 2 and 3. The experimental validation results for different power levels are presented in Figures 10 (a) to (d).

$$Q_T = V_c a_p' f, \tag{2}$$

$$Q_P = V_c a_p f. \tag{3}$$

Vc is the cutting speed (mm/min); ap' is the theoretical cutting depth (mm); ap is the actual cutting depth (mm); f is the feed rate (mm/min).

The results indicate that with an increase in laser power, the actual material removal rate gradually rises, consistent with the trend of the theoretical removal rate. At the same laser power, the minimum surface roughness of the material is observed at the optimal cutting depth determined through simulation. However, discrepancies arise between the theoretical and actual removal rates at higher laser powers, primarily due to the expanded selection range for cutting depth and increased tool wear associated with high energy. Therefore, when using higher power settings, choosing a cutting depth slightly smaller than that indicated by the simulation results is advisable. Overall, the softened layer depth obtained from temperature field simulations closely aligns with the actual machining outcomes, exhibiting a consistent trend, thus providing an effective reference for turning processes.

4. Experimental Design

In laser-assisted turning, we investigated the influences of laser power and feed speed on temperature based on the simulation of the temperature field.

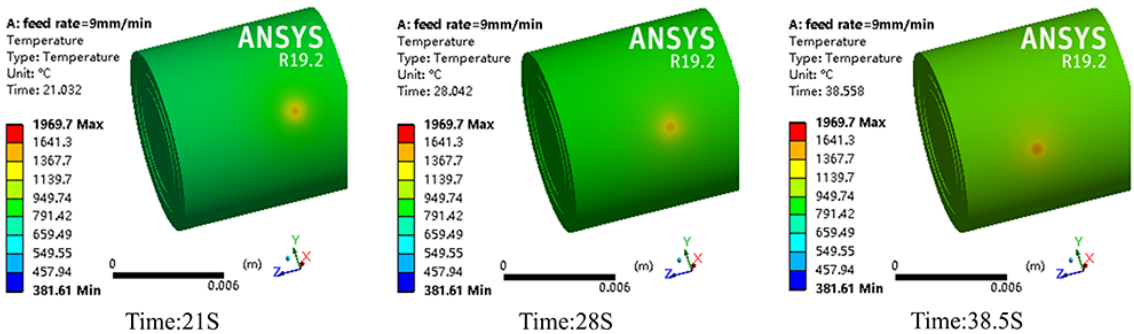

Fig. 7 Surface temperature distribution at different time points.

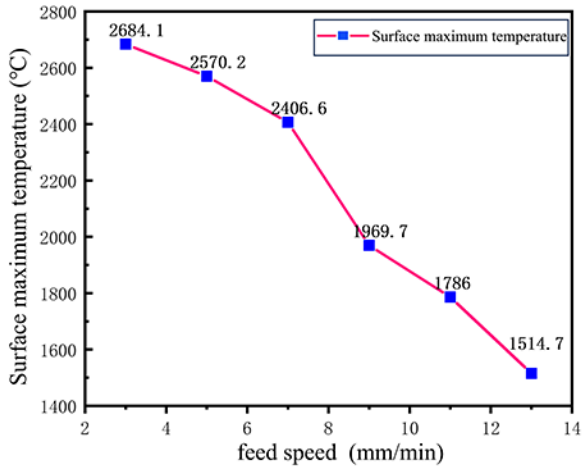

Fig. 8 The variation trend of the maximum surface temperature at different feed rates.

This simulation helped us identify the appropriate value ranges of the four key processing parameters: laser power, spindle rotational speed, depth of cut, and laser-tool distance. In the experimental design, other parameters are set as follows: turning length Lc= 10 mm, preheating time T = 30 s, spot diameter D = 1 mm, and the angle between the laser light source and the horizontal end face of tool α = 90°. On this basis, the Box-Behnken design (BBD) experiment was used to design the experimental scheme based on the response surface theory, and laser-tool distance (A), laser power (B), spindle speed (C), and cutting depth (D) were selected as the optimization parameters at the levels of -1, 0, and +1, respectively. The BBD experimental scheme of four factors and three levels was designed with the surface roughness Ra of the workpiece after processing as the response index, and the linear transformation was performed using Formula (4).

$$Z_i=\frac{X_i-X_{i0}}{V_i}\ (i=1,2,3,4). \tag{4}$$

In the formula, Z_i is the variable encoding value; X_i is the real value of the processing parameter variable; X_{i0} is the true value of the processing parameter variable 0 levels; V_i is the range of real value interval. The factor levels and coding are shown in Table 2.

To maximize the avoidance of machining errors, each group of experiments ensured that the same process was repeated 2 times for turning. When measuring the surface roughness, three positions were sampled along the feed direction at a length of 0.8 mm, and each position was repeated three times to calculate the average value.

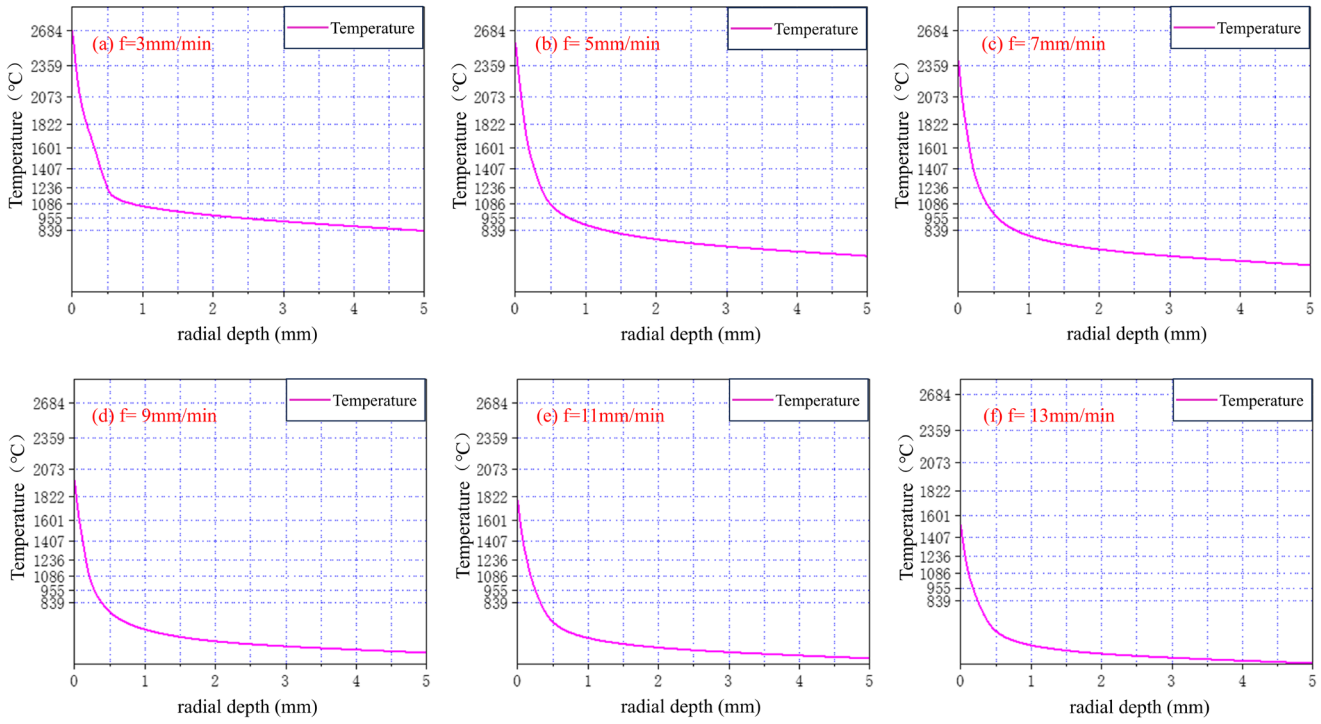

Fig. 9 Radial temperature distribution at different feed speeds.

Table 2 Response surface experimental factor levels.

Parameters	Notation	Unit	Levels of Factors		
			-1	0	+1
Laser-tool Distance (D)	A	mm	0.8	1.0	1.2
Laser Power（P）	B	W	60	112.5	165
Spindle speed（S）	C	r/min	350	650	950
Cutting depth（a_p）	D	mm	0.15	0.22	0.3

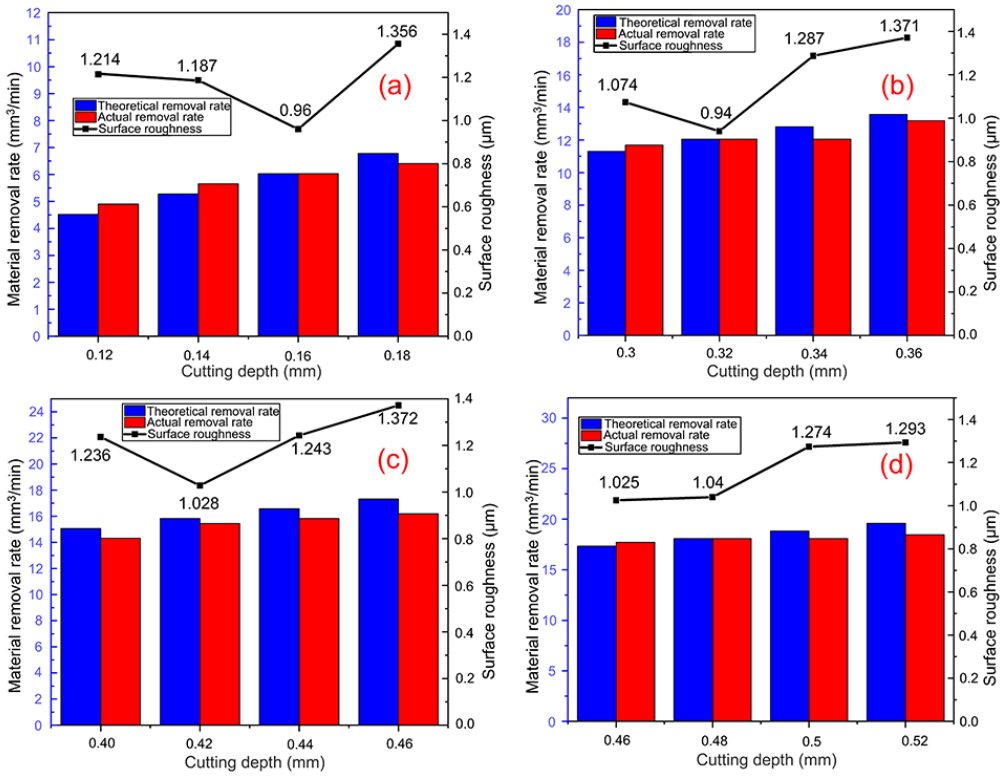

Fig. 10 Surface roughness and material removal rate measurement results.

5. Results and Discussion

5.1 Surface roughness regression model

29 groups of response surface experiments were carried out with surface roughness Ra as the response value. The experimental scheme and results are shown in Table 3. Using Design-Export 13.0 software to fit the experimental data, a response surface regression model was obtained with surface roughness as the index and four process parameters of laser-tool distance A, laser power B, spindle speed C, and cutting depth D as variables. The regression model equation is shown in formula (5) [23, 24].

$$R_1=0.8606-0.0036A+0.0261B+0.0066C+0.0556D-0.0405AB+0.0025AC-0.0503AD -0.0245BC+0.0777BD+0.0018CD+0.0533A^2+0.0560B^2+0.0513C^2+0.0933D^2, \quad (5)$$

Table 3 Experimental scheme and results.

test	*A*- laser-tool distance / (mm)	*B*- laser power / (W)	*C*- spindle speed / (r/min)	*D*- cutting depth / (mm)	*Ra*- surface roughness /(μm)
1	0	-1	0	-1	1.023
2	0	0	-1	1	1.069
3	1	-1	0	0	0.981
4	-1	0	1	0	0.967
5	0	1	-1	0	1.032
6	-1	0	0	-1	0.914
7	0	1	0	-1	0.901
8	-1	1	0	0	1.046
9	0	0	0	0	0.873
10	0	0	0	0	0.864
11	1	0	0	1	0.997
12	0	1	0	1	1.149
13	1	1	0	0	0.945
14	0	1	1	0	0.979
15	0	0	-1	-1	0.931
16	-1	-1	0	0	0.920
17	0	-1	0	1	0.960
18	0	0	0	0	0.848
19	1	0	-1	0	0.955
20	0	0	0	0	0.868
21	-1	0	-1	0	0.945
22	1	0	0	-1	0.998
23	0	-1	-1	0	0.905
24	-1	0	0	1	1.114
25	0	0	0	0	0.850
26	0	0	1	-1	0.944
27	0	0	1	1	1.089
28	1	0	1	0	0.987
29	0	-1	1	0	0.950

5.2 Regression model analysis

As shown in Figure 11, the normal distribution diagram of the residuals of the surface roughness prediction model is shown. It can be concluded from Figure 11 that the residual normal distribution of the model is distributed on a straight line, which indicates that the predicted value is close to the actual value, so the predicted value of the surface roughness of the model can be in good agreement with the actual value.

When the *P* value was less than 0.05, the corresponding independent variable item had a significant effect on the dependent variable item. When the *P* value was less than or equal to 0.0001, the corresponding independent variable item had a highly significant effect on the dependent variable item.

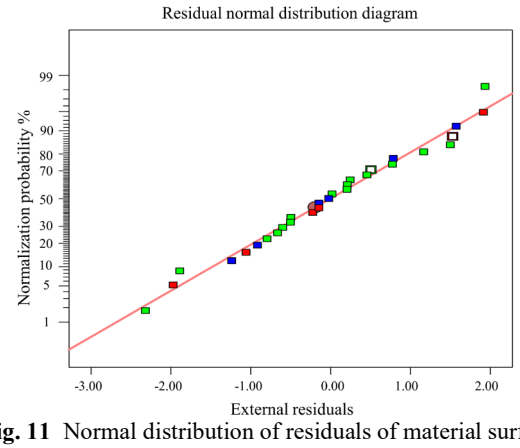

Fig. 11 Normal distribution of residuals of material surface roughness.

When the P value was greater than 0.05, the independent variable item had no significant effect on the dependent variable item. It can be seen from Table 4 that the F value of the regression model is 38.32, and the P value is less than 0.0001, indicating that the regression model is significant, that is, the regression equation established between surface roughness and various processing parameters is highly significant. The *F* value of the lack of fit is 3.12, and t the test value of the *P* value is greater than 0.05, indicating that the degree of lack of fit is not obvious. The multivariate correlation coefficient R^2 is 0.9764, and the corrected R_{Adj}^2 is 0.9491, indicating that the regression model can explain 94.91 % of the response value. The influence of cutting depth and laser power on the surface roughness is highly significant and significant respectively. Therefore, the order of the influence of each factor on the surface roughness in the laser-assisted turning Al_2O_3 experiment is cutting depth, laser power, spindle speed, and laser-tool distance. In the interaction effect term, the P-value of AB (laser-tool distance - laser power), AD (laser-tool distance - cutting depth), BC (laser power - spindle speed), and BD (laser power - cutting depth) is less than 0.05, which means that the interaction effect of these four groups was significant.

5.3 Interaction Analysis of Surface Roughness

Based on the regression model equation of surface roughness and the results of the test scheme, using the control variable method, the above highly significant interaction AB (laser-tool distance - laser power), AD (laser-tool distance - cutting depth), BC (laser power - spindle speed), and BD (laser power - cutting depth) were selected to make 3D response surface images and contour maps on surface roughness, as shown in Figure 12.

Figure 12 (a) and Figure 11 (b) are the 3D surface plots and contour plots of the interaction between laser-tool distance and laser power. When the spindle speed and the cutting depth remain unchanged at the center value, the surface roughness of the material increases obviously by using the maximum laser power with a small distance and the maximum laser-tool distance with a small laser power. Therefore, a lower surface roughness can be obtained by using a smaller laser power and distance. This is because the great laser power makes the material heat up quickly, and the smaller distance will make part of the heat quickly transferred to the tooltip, making the tool wear drastically; the large distance makes the tool into the turning time lag, with the lower laser power cannot reach the softening conditions of the plastic turning. From the graphical observation and analysis, it is concluded that the use of 0.9~1.1 mm laser-tool distance with a laser power of 100~120 W can obtain a lower surface roughness.

Table 4 Analysis of variance of surface roughness regression model.

Source	Sum of squares	DOF	Mean Square	F-value	P-value	
Model	165×10^{-3}	14	118×10^{-4}	38.32	<0.0001	significant
A	2×10^{-4}	1	2×10^{-4}	497×10^{-3}	0.4913	
B	82×10^{-4}	1	82×10^{-4}	26.47	0.0001	
C	5×10^{-4}	1	5×10^{-4}	1.69	0.2151	
D	371×10^{-4}	1	371×10^{-4}	120.21	<0.0001	
AB	66×10^{-4}	1	66×10^{-4}	21.27	0.0004	
AC	1×10^{-4}	1	1×10^{-4}	0.0811	0.7800	
AD	101×10^{-4}	1	101×10^{-4}	32.75	<0.0001	
BC	24×10^{-4}	1	24×10^{-4}	7.79	0.0145	
BD	242×10^{-4}	1	242×10^{-4}	78.40	<0.0001	
A^2	184×10^{-4}	1	184×10^{-4}	59.71	<0.0001	
B^2	204×10^{-4}	1	204×10^{-4}	66.04	<0.0001	
C^2	171×10^{-4}	1	171×10^{-4}	55.31	<0.0001	
Residual	43×10^{-4}	14	3×10^{-4}			
Lack of Fit	38×10^{-4}	10	4×10^{-4}	3.12	0.1423	not significant
Pure Error	5×10^{-4}	4	1×10^{-4}			
Cor Total	169×10^{-3}	28				
			R^2=0.9746	R_{Adj}^2=0.9491		

Figure 12 (c) and Figure 12 (d) are the 3D surface plots and contour plots of the interaction between laser-tool distance and cutting depth. When the laser power and spindle speed are fixed in the middle value, the surface roughness of the material is significantly increased by using a very large laser-tool distance with a very small amount of cutting depth or using a large amount of cutting depth within the range of distance. The reason is that the great laser-tool distance makes the turning process lag behind the softening process, the temperature produces a fallback deterioration, with a very small amount of cutting depth makes the turning force of the tool not enough; too large amount of cutting depth will increase the depth of turning so that the turning force compared to the low cutting depth increases significantly if the smaller distance is used with the inevitable result of high temperature will lead to excessive wear of the tool, if the use of a large distance with the tool in the brittle environment machining. From the observation and analysis of the diagram, it is concluded that the lower surface roughness can be obtained by using the laser-tool distance of 0.9 ~ 1.1 mm and the cutting depth of 0.21 ~ 0.23 mm.

Figure 12 (e) and Figure 12 (f) are the 3D surface plots and contour plots of the interaction between laser power and spindle speed. Surface roughness increases with increasing laser power and spindle speed when the laser-tool distance and cutting depth are fixed at constant center values. The reason is that when the spindle speed is faster and the laser power is smaller, the heat energy released by the laser heat source itself is small. At the same time, the spindle speed is too fast to make the laser beam irradiate the workpiece surface for a short time, and the material cannot be fully softened. The high-energy laser beam released by a larger laser power causes the surface of the material to heat up rapidly. The high temperature causes the melting of some areas of the material, and the flow of the surface particle distribution causes the surface flatness to be destroyed. Comprehensive analysis shows that a lower surface roughness can be obtained when the laser power is 100-120 W and the spindle speed is 500-700 r / min.

Figure 12 (g) and Figure 12 (h) are the 3D surface plots and contour plots of the interaction between laser power and cutting depth. When the laser-tool distance and spindle speed are fixed at a constant center value, higher laser power, and larger cutting depth, as well as lower laser power and smaller cutting depth, do not result in small surface roughness. The reason for this is that the laser is the only heat source, and when the backdraft exceeds the actual depth of the softened layer, it can lead to turning into the unsoftened material layer, thus preventing the achievement of small surface roughness. When the laser power is too low, the heat energy released by the laser beam is very small, and the plastic removal cannot be guaranteed even if the cutting depth is very small. Excessive cutting depth makes the turning force increase significantly, the high-temperature effect of a high-energy laser heat source is superimposed, and the tool wear is severe. In summary, a cutting depth of 0.21~0.23 mm with a laser power of 100~120 W can be used to obtain a lower surface roughness.

6. Optimization and verification

6.1 Optimization and verification of the response surface method

The optimal parameter ranges of the above four process parameters obtained from the analysis were converted into coded values using Equation (4) to be brought into Regression Equation (5), and aiming at the minimum surface roughness of the processed alumina ceramic, according to the actual situation of the laser heating system, CNC machine tools and CBN tools, the parameters of each processing factor are obtained as follows: the laser-tool distance is 0.95 mm, the laser power is 112 W, the spindle speed is 635 r / min, and the cutting depth is 0.22 mm.

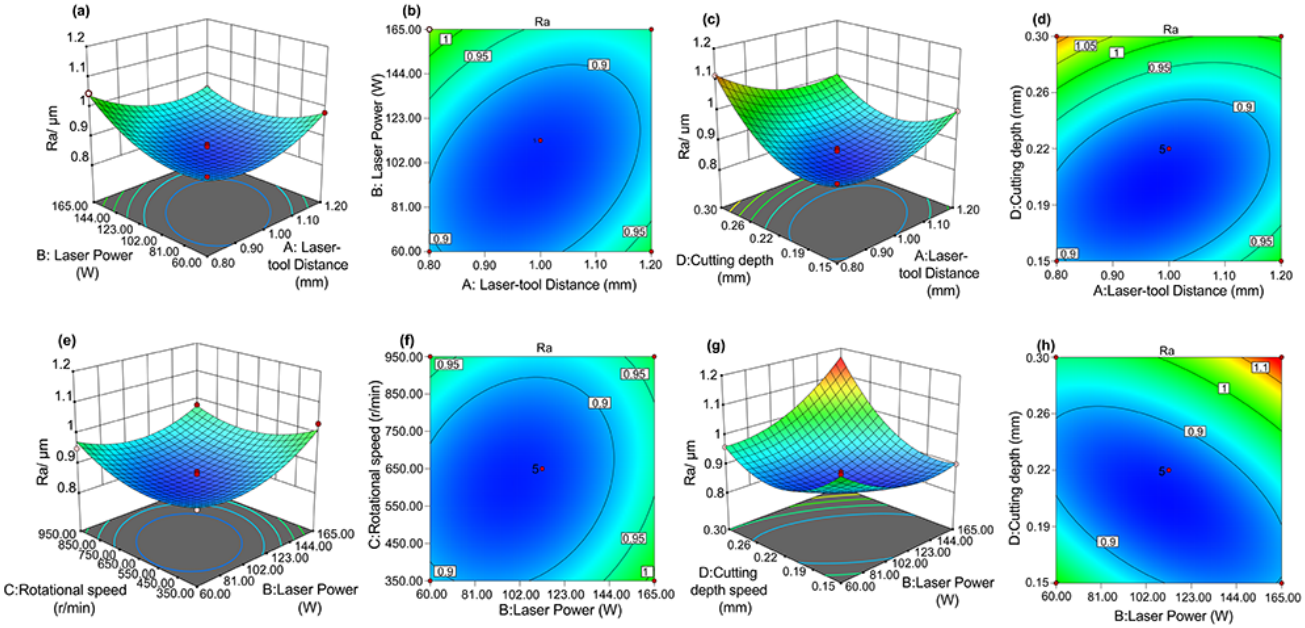

Fig. 12 The interaction effect of process parameters on surface roughness in response surface.

To accurately reflect the optimized surface roughness results, three sets of repeated experiments were conducted using this combination of parameters. For each set of experiments, two measurement points were randomly selected to assess the surface roughness. The obtained surface roughness results are presented in Table 5, with the corresponding surface profile curves illustrated in Figure 13. After processing with the optimized parameters, the average surface roughness (Ra) was measured at 0.816 μm, with a minimum value of 0.806 μm. Compared to the results from Test Scheme No. 12, the Ra value decreased by 0.343 μm, representing a reduction of 29.8%. Similarly, compared to Test Scheme No. 18, the Ra value decreased by 0.042 μm, corresponding to a reduction of 5.0%.

Meanwhile, to show the significant difference in surface forming quality between brittle processing and plastic processing, the conventional turning of alumina ceramics is carried out by using the combined parameters of tool and spot spacing 0.95 mm, spindle speed 635 r / min and back cutting amount 0.22 mm, the surface profile is shown in Figure 14. Conventional turning of brittle machining of the resulting surface flatness is poor, the peaks and valleys of the contour surface of the difference are large, and there are obvious surface fractures, pits, and other defects, these defects are due to brittle machining of the high hardness of the larger turning force caused by the brittle fracture occurs when interacting with tools.

6.2 Surface morphology

In Figure 15, (a) ~ (d) is the original grinding surface, conventional turning surface, pre-optimized, and post-optimized machining surface of alumina ceramics, respectively. It can be observed that compared with the brittle machined surface in Figure 15 (a) and (b), the surface defects such as tool scratches, material fractures, and large-area continuous pits on the LAM plastic turning surface are significantly reduced, and the surface flatness of the material is further improved after optimization. Even when starting with a rough ground surface (Ra 1.5–2.0 μm), LAM can reduce the surface roughness to the Ra 0.8 μm level in a single-step process, significantly reducing reliance on traditional multi-step procedures (such as rough grinding → fine grinding → polishing). During the rough machining stage, LAM enables plastic domain removal of brittle ceramics, preventing the accumulation of surface defects caused by brittle fracture in conventional turning. This provides a more uniform substrate for subsequent semi-finishing processes.

6.3 Tool wear

In laser-assisted turning, the additional heat provided by the laser beam concentrates in the cutting area, resulting in an elevated temperature on the tool's rake face and consequently accelerating tool wear. This study selects the rake face with the most pronounced wear as the measurement indicator for observation purposes. The optimal parameters were selected for further processing, with laser power incrementally set at 60 W, 90 W, 112 W, 120 W, and 150 W. For traditional turning, the best-optimized parameters without laser power were similarly selected for processing to observe tool wear. The figure below illustrates the condition of the tool's wear.

At a laser power of 112 W, the tool wear value is 64.1 μm, which is the minimum, indicating that the optimal machining parameters result in minimal tool damage. In comparison, traditional turning exhibits a tool wear value of 152.1 μm, demonstrating that laser-assisted turning is more effective and better for tool protection. As laser power increases, the tool wear value generally shows a decreasing trend; however, at 150 W, the wear value increases. This is attributed to the additional energy from the laser beam concentrating on the tool, raising its temperature and accelerating tool wear.

Table 5 Experimental results after optimization of parameters.

Text 1		Test 2		Test 3		average value
0.806μm	0.819μm	0.810μm	0.812μm	0.825μm	0.822μm	0.816μm

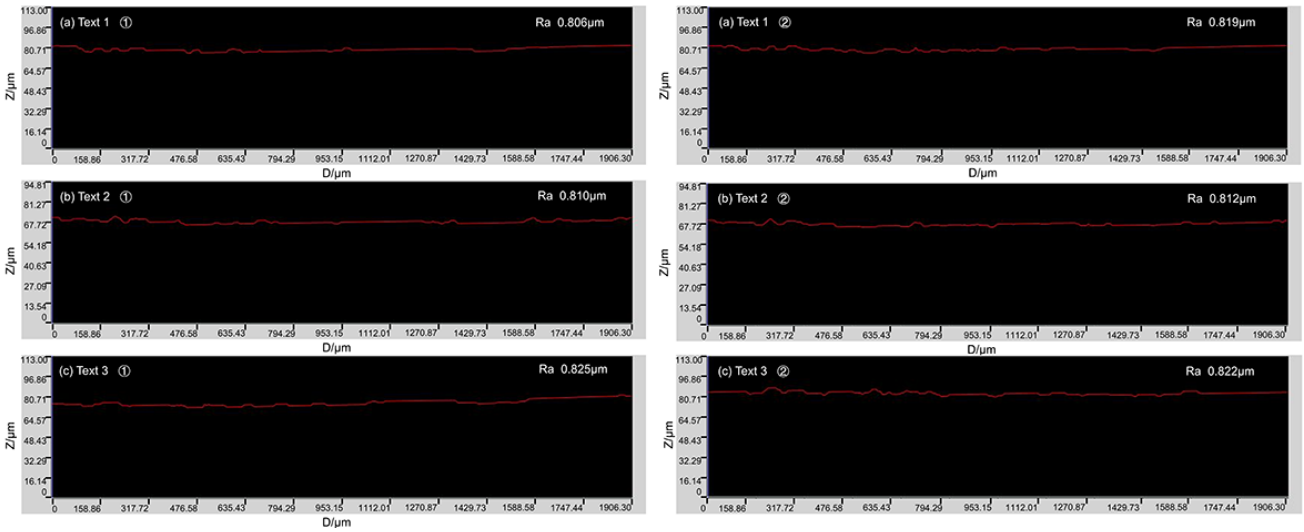

Fig. 13 Surface profile curve for optimization test.

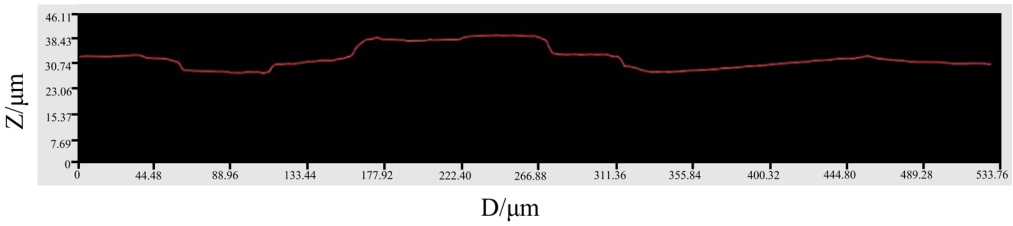

Fig. 14 Surface Profile Curves for Conventional Turning.

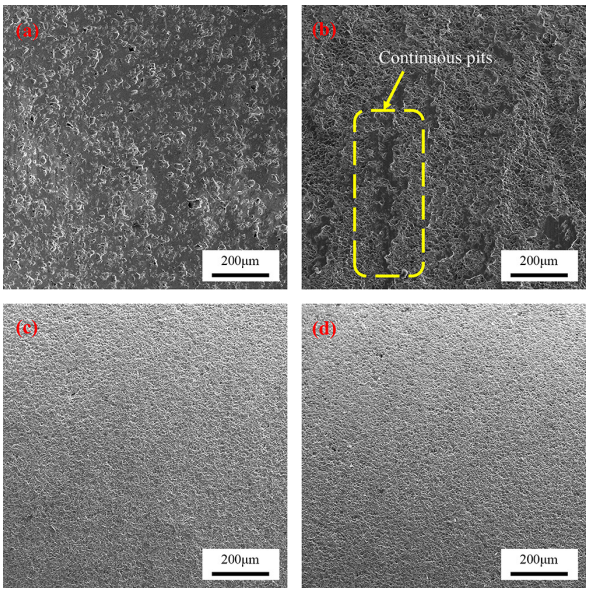

Fig. 15 Surface morphology under different processing methods. (a) Original grinding surface, (b) Conventional turning surface, (c) Test Scheme No. 18, (d) Optimize the test surface.

7. Conclusions

Based on clarifying the principle of laser-assisted turning, this paper studies and analyzes the influence law of processing factors through experimental research, and finally optimizes the parameters. The specific results are summarized as follows:

(1) The influence of laser power and feed rate on temperature was investigated through temperature field simulations. The feasibility of the simulation was validated by comparing the theoretical material removal rate with the actual material removal rate. Using laser-tool distance, laser power, spindle speed, and cutting depth as variables, a 29-group experimental investigation was carried out using the response surface approach to create a regression model for surface roughness. The residuals and ANOVA results demonstrated that the model fits well.

(2) Surface roughness is used as an indicator to analyze the influence of laser-tool distance, laser power, spindle speed, and cutting depth on LAM machining results, and the surface roughness of the factors is determined in the following order: cutting depth > laser power > spindle speed > laser-tool distance.

(3) The surface roughness was optimized by the response surface optimization parameter method. The optimal processing parameters are as follows: laser-tool distance is 0.95 mm, laser power is 112 W, spindle speed is 635 r / min, and cutting depth is 0.22 mm. After processing with the optimized parameters, the minimum surface roughness Ra reaches 0.806 μm, and the average value reaches 0.816 μm.

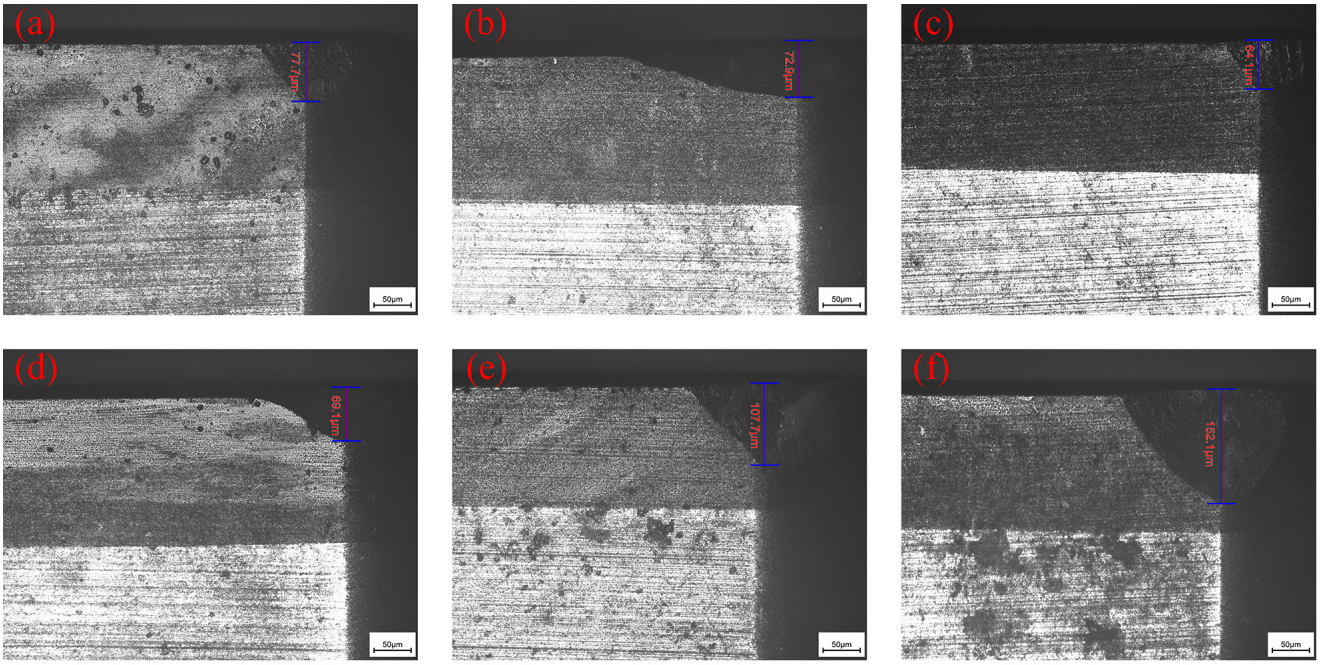

Fig. 16 (a) ~ (e) are 60W, 90W, 112W, 120W, 150W laser power processing, (f) is a traditional processing.

(4) By observing and comparing the surface morphology and tool wear of Al_2O_3 ceramics under different processing methods, it is demonstrated that the surface quality and tool wear associated with laser-assisted machining (LAM) are significantly superior to those observed in conventional turning. Through the element analysis of the material surface, it is proved that the LAM plastic processing does not cause adhesion between the tool and the ceramic due to the abnormal wear of the tool, to ensure that no impurities are produced after processing.

Author contribution

This method was proposed by Caizhou Xin and Haiyun Zhang. The experiment was designed by Caizhou Xin and was conducted by Zhiguo Geng, Yanan Guo, Zengbo Zhang, Jinjian Zhang, Xu Miao and Xingang Han. The preparation of the original manuscript of the paper was completed by Caizhou Xin. The review and editing work was completed by Yugang Zhao and Haiyun Zhang. All authors read and approved the final manuscript.

Funding

National Natural Science Foundation of China (51875328); Natural Science Foundation of Shandong Province (ZR2019MEE013, ZR2021ME159).

Acknowledgments

Thanks to the National Natural Science Foundation of China and the Natural Science Foundation of Shandong Province for help identifying collaborators for this work.

Data availability

Data underlying the results presented in this paper are not publicly available at this time but may be obtained from the authors upon reasonable request.

Declarations

Consent to participate Not applicable.
Ethics approval Not applicable.
Consent for publication Not applicable.
Conflict of interest The authors declare no conflicts of interest.

References

[1] M.F. Hu, J. Xie, H.H. Su, and J.N. Liu: Int. J. Adv. Manuf. Technol., 94, (2018) 2919.
[2] Z. Ma, Q. Wang, J. Dong, Z. Wang, and T. Yu: Precis. Eng., 72, (2021) 798.
[3] V. M. Sglavo: Front. Ceram., 1, (2023) 1136720.
[4] J.I. Arrizubieta, F. Klocke, S. Gräfe, K. Arntz, and A. Lamikiz: Procedia Eng., 132, (2015) 639.
[5] H. Ding and Y.C. Shin: Int. J. Mach. Tools Manuf., 50, (2009) 106.
[6] G. Germain, P. Dal Santo, and J.-L. Lebrun: Int. J. Mach. Tools Manuf., 51, (2011) 230.
[7] S.H. Masood, K. Armitage, and M. Brandt: Int. J. Mach. Tools Manuf., 51, (2011) 450.
[8] C. Zhang and Y.C. Shin: Int. J. Mach. Tools Manuf., 42, (2002) 825.
[9] M.M. Kashani, M.R. Movahhedy, M.T. Ahmadian, and R.S. Razavi: Int. J. Adv. Manuf. Technol., 92, (2017) 2929.
[10] F. Zhao, W.Z. Bernstein, G. Naik, and G.J. Cheng: J. Clean. Prod., 18, (2010) 1311.
[11] Y. Wang, L.J. Yang, and N.J. Wang: J. Mater. Process. Technol., 129, (2002) 268.
[12] H. Mohammadi, D. Ravindra, S.K. Kode, and J.A. Patten: J. Manuf. Process., 19, (2015) 125.
[13] M.V. Kannan, P. Kuppan, A.S. Kumar, K.R. Kumar, and J.J.R. Jegaraj: Procedia Eng., 97, (2014) 1647.
[14] S.M. Langan, D. Ravindra, and A.B. Mann: Precis. Eng., 56, (2019) 1.
[15] Y. Jin, B. Wang, P. Ji, Z. Qiao, D. Li, and F. Ding: Int. J. Adv. Manuf. Technol., 124, (2023) 69.
[16] C. Cao, Y. Zhao, J. Meng, D. Dai, Q. Liu, G. Liu, H. Zhou, Z. Song, H. Zhang, and X. Zhang: Int. J. Adv. Manuf. Technol., 125, (2023) 4467.
[17] W. Habrat, K. Krupa, A.P. Markopoulos, and N.E. Karkalos: Int. J. Adv. Manuf. Technol., 115, (2020) 759.
[18] H.-I. Jeong and C.-M. Lee: Opt. Laser Technol., 142, (2021) 107208.
[19] V.P. Saradhi, V. Shashank, P.S. Teja, G. Anbarasu, A. Bharat, and T. Jagadesh: Mater. Today: Proc., 5, (2018) 20343.
[20] H. Song, J. Dan, X. Chen, J. Xiao, and J. Xu: Int. J. Adv. Manuf. Technol., 97, (2018) 267.
[21] C.-W. Chang and C.-P. Kuo: Int. J. Mach. Tools Manuf., 47, (2007) 452.
[22] R. Bejjani, B. Shi, H. Attia, and M. Balazinski: CIRP Ann., 60, (2011) 61.
[23] H. Song, J. Dan, J. Du, G. Ren, J. Xiao, and J. Xu: Silicon, 11, (2019) 3049.
[24] H. Song, J. Dan, J. Li, J. Du, J. Xiao, and J. Xu: J. Manuf. Process., 38, (2019) 9.

(Received: November 18, 2024, Accepted: April 30, 2025)